WDS'05 Proceedings of Contributed Papers, Part II, 362–367, 2005. *ISBN 80-86732-59-2 © MATFYZPRESS*

2D PIC Simulation of the DC Discharge in Cylindrical Magnetron

A. Marek, P. Kudrna, I. Picková, M. Holík, O. Bilyk, and M. Tichý

Charles University, Faculty of Mathematics and Physics, Prague, Czech Republic.

Abstract. We report on 2D Particle-In-Cell (PIC) simulations of dc magnetized discharge. Simulations were made by XOOPIC code developed on the University of California, Berkeley. Results of the simulation are compared with experimental data obtained by Langmuir probe and emissive probe diagnostics in cylindrical magnetron device.

Introduction

PIC method of plasma simulation is widely used in plasma physics research because of its ability to solve wide range of problems in kinetic approach. Regarding to description of PIC method we refer to [*Birdsall et al.*, 1995]. This work is focused on PIC simulations of dc discharge in cylindrical magnetron device. Magnetrons are used in industry e.g. for thin film layer coating and etching. Many magnetron configurations are used. In our research we concentrate on cylindrical magnetron device because its symmetry and simple magnetic field arrangement enables relatively simple theoretical description and makes understanding of processes in weakly magnetized plasma easier by avoiding effects of nonhomogenous magnetic field. We study the influence of the magnetic field on discharge parameters and the PIC model can contribute to its description.

Experimental system - cylindrical magnetron

Scheme of the cylindrical magnetron device used for experimental research in our laboratory is depicted in Figure 1 and is described in detail in [*Passoth et al.*, 1997] so that only its overview will be given at this place: Cylindrical magnetron consists of grounded stainless steel tube (anode) and water cooled cathode at its axis. Discharge area (12 cm long) is constrained by two metallic limiters connected to the cathode potential. Plasma in magnetron is confined by homogeneous magnetic field parallel to axis. It is created by couple of magnetic coils and can vary up to 40 mT. Magnetron usually operates in noble gases at pressures 1 −10 Pa. Ultimate pressure of the system is in the order of 10^{-3} Pa. Plasma parameters can be determined by means of electrical probes placed in vacuum feedthrough in the central plane of magnetron. Some experimental data presented in this contribution are obtained in similar cylindrical magnetron (see e.g. [*Holík et al.*, 2004]) that differs from that one described here in length of discharge area (30 cm instead of 12 cm) and also in electrodes diameters (anode diameter is 56 mm and cathode diameter is 18 mm). Let us to denote these two magnetrons like "longer" and "shorter" magnetron for easier handling in this text. Shorter magnetron's dimensions are given in Figure 2.

PIC model of the magnetron

For simulations we applied XOOPIC code [*Verboncoeur et al.*, 1995] developed on the University of California, Berkeley. Scheme of the region used for 2D PIC model of discharge in cylindrical magnetron is depicted in Figure 2. Due to symmetry of the discharge area it is possible to place reflecting boundary at the middle of the magnetron and reduce computational effort in this way (i.e. we simulated only half of discharge area – from the center of magnetron to the left limiter). For simulations we used grid equidistant in both directions. Discharge was powered by constant voltage source in PIC model in contrast to experiment operating in constant current mode. Following interactions were considered in argon discharge: elastic collisions , excitation and ionization for electrons and elastic collisions and charge exchange interaction for single charged argon ions.

2D code is needed for computational model of the discharge in cylindrical magnetron, because discharge is not homogeneously distributed along the whole discharge region. Simulations were relatively computational consuming. That is because conditions have to be fulfilled that ensure stable and physically correct solution. [*Vahedi et al.*, 1993] formulated such conditions as follows: 1.) cell length smaller or comparable with Debye length (that is in order of tens of μm in magnetron), 2.) reasonable number

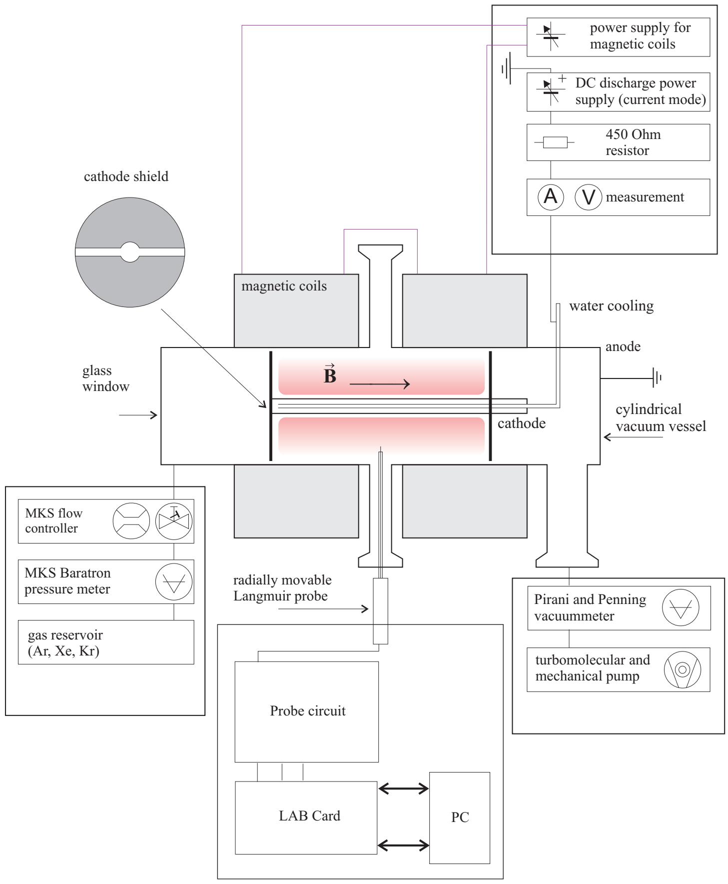

Figure 1. Schematic diagram of cylindrical magnetron apparatus.

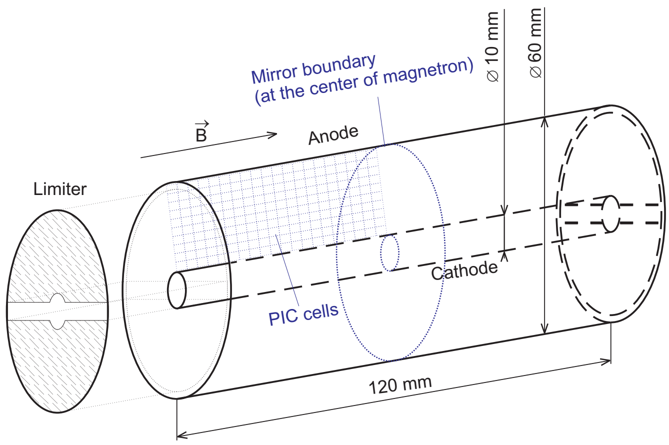

Figure 2. Scheme of region for 2D PIC simulation of discharge in the ”shorter” magnetron.

of simulating superparticles in cell (optimally 10-50 per cell) and 3.) time step restrictions: time step must resolve processes on plasma frequency and particles mustn't fly over more than one cell in one time step.

Results of the PIC model

An example of results of the simulation is depicted in Figure 3. Presented data were obtained in simulation, where the cell length was comparable with Debye length (i.e. 1250 x 500 cells). Timestep was $\Delta t = 10^{-11}$ s for electrons, for ions double. Other simulation conditions are given in the caption

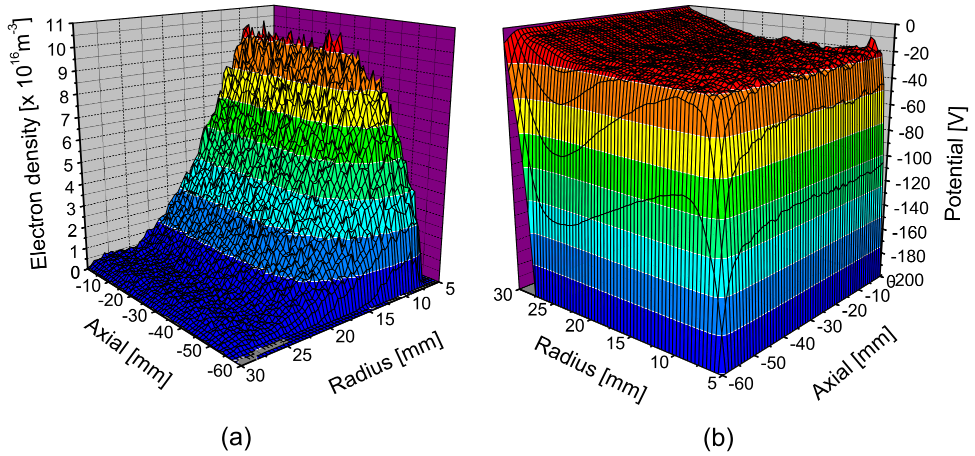

Figure 3. XOOPIC simulation results of Argon discharge in magnetron at $p = 4$ Pa, $B = 20$ mT, $U_{Cathode} = -200$ V. Data are from snapshot taken at discharge time $t = 6,4.10^{-7}$ s. Density profile used for initial condition was obtained from former simulation with rougher computational grid. Zero of axial coordinate denotes center of magnetron; $r_{Anode} = 30$ mm; $r_{Cathode} = 5$ mm. Cell length is comparable with Debye length (i.e. 500 x 1250 cells); time step $\Delta t = 10^{-11}$ s for electrons, for ions double. (a) electron density profile, (b) potential profile (for better view 90° clockwise rotated).

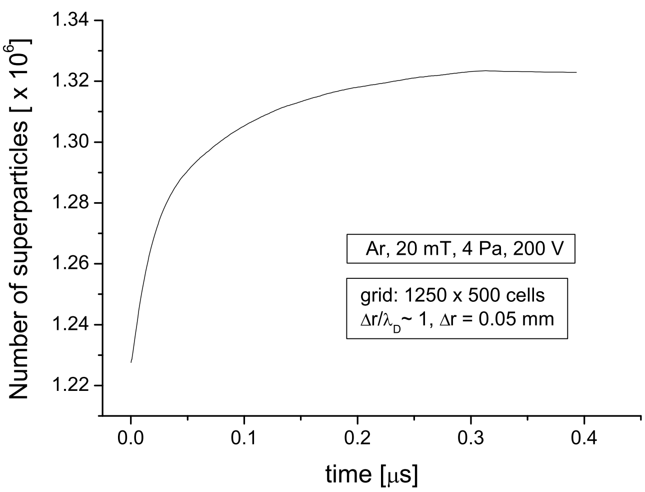

Figure 4. Development of the number of superparticles in simulation with grid with 500 x 1250 cells.

of Figure 3. The temporal development of the number of superparticles in this simulation is depicted in Figure 4. One superparticle represented in our simulation 7.10^5 real particles in plasma. Temporal development of the number of superparticles is one of important criteria ensuring stable solution in models of the steady state glowing discharges - the number of superparticles in simulation should be stabilized in dynamical equilibrium in such a case. Stabilized state of the number of superparticles was reached in presented simulation.

In our previous simulations with rougher computational grid (see Figure 5) rose the number of superparticles monotonously during simulation at the same discharge conditions (i.e. discharge in Argon at $p = 4$ Pa, $B = 20$ mT, $U = -200$ V). Cell length was in that case approximately three times bigger

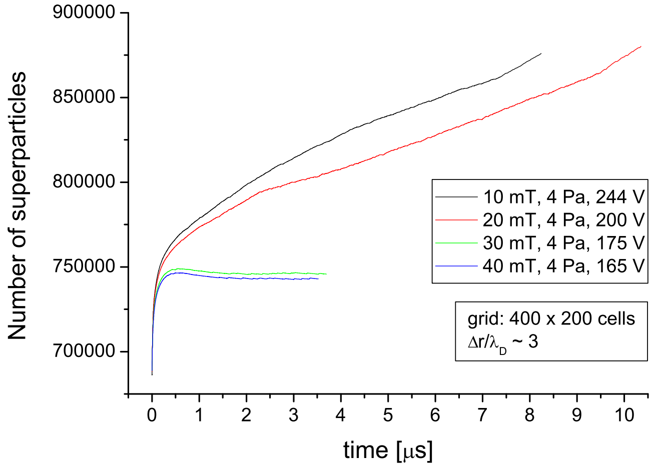

Figure 5. Development of the number of superparticles in simulation with rougher grid for different discharge conditions. Applied discharge voltage was chosen proportionally to experiment.

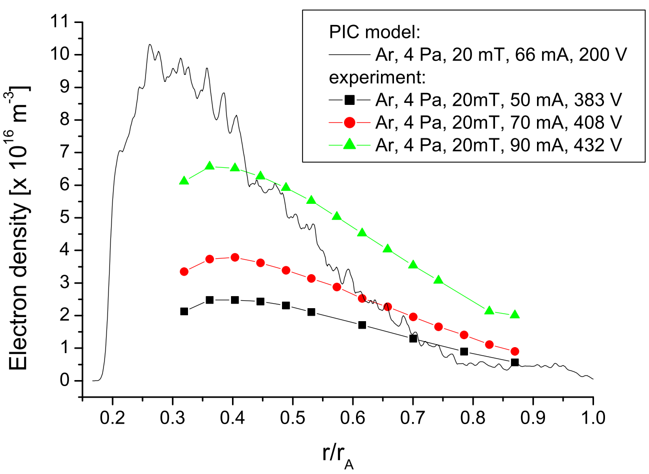

Figure 6. Comparison of computed radial electron density profile with data obtained via Langmuir probe; r_A denotes anode radius. Discharge current in PIC model was determined by averaging over interval 0.2 μs of discharge.

than Debye length. It means, first condition given in [*Vahedi et al.*, 1993] was not fulfilled. These simulations were made at begining because of lower computational requirements of simulation. However, note an interesting stabilizing effect of magnetic field on discharge illustrated in Figure 5. Explanation is unclear. Simultaneous change of magnetic field and applied discharge voltage makes explanation more complicated.

Comparison with experiment will be given for the recent one simulation with more precise grid.

Comparison with experiment

Computed radial electron density profile is compared in Figure 6 with experimental data obtained via Langmuir probe in the central plane of magnetron. Maximum of electron density profile is shifted towards cathode in comparison with Langmuir probe data and falls faster than in experiment.

Potential profile obtained in simulation is depicted for three different axial positions in Figure 7. We can see relatively broad, well formed region of positive column, where potential remains almost constant,

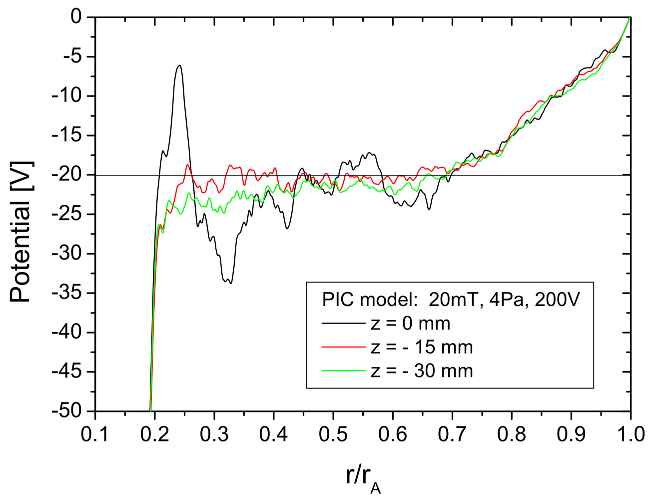

Figure 7. Detail of computed plasma potential profile at three different axial positions; r_A denotes anode radius, $z = 0$ is position in the central plane of the magnetron.

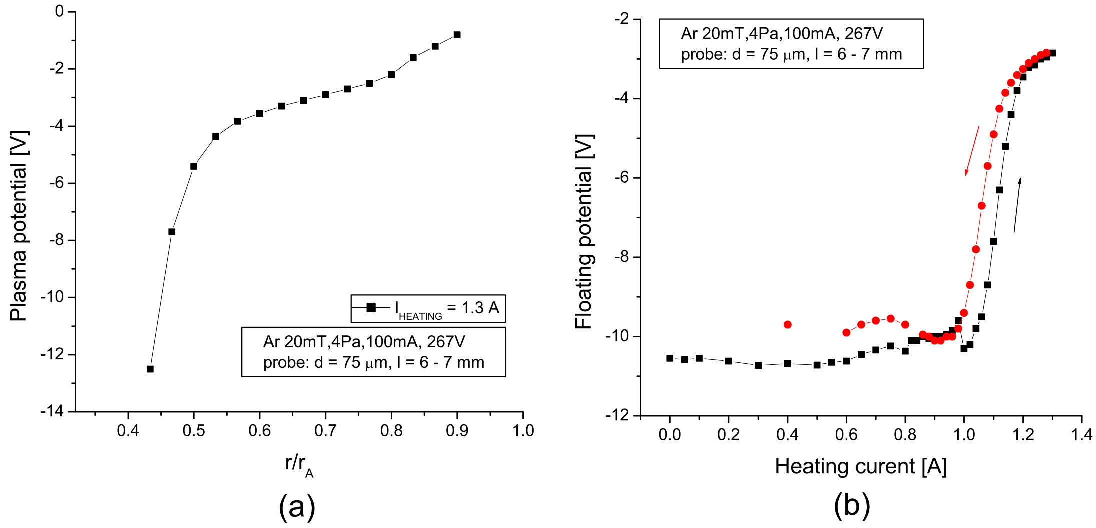

Figure 8. Emissive probe measurements. (a) plasma potential profile in magnetron (b) determination of operating point of emissive probe.

moderate anode fall and steep cathode potential fall . Noisy character of potential is caused by rather lower number of superparticles in simulation. In order to increase confidence in experimental data the computed plasma potential profile can be also compared with data obtained by emissive probe in "longer" magnetron that are depicted in Figure 8(a). Emissive probe diagnostic enables to measure directly plasma potential without any additional data processing, because floating potential of strongly emitting probe approaches the plasma potential (the difference of the order of kT_e/e is due to the space charge effect near the probe [*Ye et al.*, 2000]). Sufficient probe heating current(i.e. operating point of emissive probe) was set according to the Figure 8(b). Emissive probe data corresponded very well with plasma potential profile obtained formerly from Langmuir probe measurements at the same experimental conditions: potential drop in positive column was only few volts as well as potential drop in anode region, that was formed in relatively narrow region near the anode. We can observe, that in computed plasma potential profile (Figure 7) the anode fall is bigger than in experiment and reaches deeper into the discharge region.

Discusion

We suggest several explanations of the discrepancy between experiment and our PIC model. At first, simulation time could be too short for proper redistribution of slower particles (ions) on their steady state positions, although we tried to minimalize this effect by starting the simulation from the expected density profiles obtained in former simulation. Next, results can be affected also by rather low number superparticles per cell – used because of our restricted memory facilities – or the computational grid was not be still fine enough. Finally, the discrepancy can be partially caused by neglecting of some important interactions in model. Such an interaction could be the stepwise ionization of the Argon metastable $1s_5$, that was not included in our model. Radial density profiles of excited Argon atoms were measured in our device by means of infrared absorption spectroscopy for three of four first excited levels by C. Csambal [*Porokhova et al.*, 2002]. From measurements follows that the population density of Argon metastable $1s_5$ is in the same order as plasma density. From this reason an effect of stepwise ionization could be also nonnegligible.

Conclusion

In this contribution we presented results of our 2D PIC simulations of the dc magnetized discharge in the cylindrical magnetron device. Simulations were realized by using XOOPIC code developed at the University in Berkeley, USA. In contrast to our former simulations we obtained solution with stabilized number of superparticles in simulation. We compared this solution with experimental data measured in the cylindrical magnetron partially in laboratory at the Charles university in Prague, Czech republic and partially at the EMA University in Greifswald, Germany. Discrepancy of computed results from experimental showed that our 2D PIC model will need further improvement.

Acknowledgments. The work was financially supported by Czech Science Foundation, grants 202/03/H162, 202/03/0827 and 202/04/0360, by project COST action 527 and by EURATOM. This work is a part of the research plan MSM 0021620834 that is financed by the Ministry of Education of the Czech Republic. Thanks are also due to University of Greifswald, Germany, which provided us with the cylindrical magnetron system.

References

Birdsall, C.K., A.B. Langdon, Plasma physics via computer simulation, *Mc Graw-Hill* 1995,*Adam-Hilger* 1991.

Holík, M., O. Bilyk, A. Marek, P. Kudrna, J.F. Behnke, M. Tichý, 2D experimental studyof the plasma parameter variations of the magnetically sustained dc discharge in cylindrical symmetry in Argon, *Contrib. Plasma Phys.*, 44, 613-618, 2004.

Passoth, E., P. Kudrna, C. Csambal, J.F. Behnke, M. Tichý and V. Helbig, An experimental study of plasma density determination by a cylindrical Langmuir probe at different pressures and magnetic fields in a cylindrical magnetron discharge in heavy rare gases, *J. Phys. D: Appl. Phys*, 30, 1763-1777, 1997.

Porokhova, I.A., Y.B. Golubovskii, C. Csambal, V. Helbig, C. Wilke, J.F. Behnke, Nonlocal electron kinetics and excited state densities in a magnetron discharge in argon, *PHYSICAL REVIEW E 65*, Art. No. 046401 Part 2B, 1-10, 2002.

Vahedi, V., G. DiPeso, C.K. Birdsall, M.A. Lieberman, T.G. Roghlien, Capacitive RF discharges modelled by particle-in-cell Monte Carlo simulation. I: analysis of numerical techniques *Plasma Sources Sci. Technol.*, 2, 261-272, 1993.

Verboncoeur, J.P., A.B. Langdon and N.T. Gladd, An Object-Oriented Electromagnetic PIC Code,*Comp. Phys. Comm.*, 87, 199-211, 1995.

Ye, M. Y., S. Takamura, Effect of space-charge limited emission on measurements of plasma potential using emissive probes *Phys. Plasmas*, 7, 3457-3463, 2000.